Environmental Science and Pollution Research (2023) 30:60976–60993
https://doi.org/10.1007/s11356-023-26412-8

RESEARCH ARTICLE

Phytochemical profiling, in vitro antioxidants, and antidiabetic efficacy of ethyl acetate fraction of *Lespedeza cuneata* on streptozotocin-induced diabetic rats

Arokia Vijaya Anand Mariadoss[1,2] · SeonJu Park[3] · Kandasamy Saravanakumar[1] · Anbazhagan Sathiyaseelan[1] · Myeong-Hyeon Wang[1]

Received: 3 September 2021 / Accepted: 8 March 2023 / Published online: 12 April 2023

Abstract

In the recent past, phytomolecules are exponentially applied in discovering the antidiabetic drug due to less adverse effects. This work screened the active solvent fraction of *Lespedeza cuneata* based on the phytochemical, enzyme inhibition, and antioxidant properties. The antioxidant efficacy of the different fractions of the *L. cuneata* was assessed by 1,1-diphenyl-2-picrylhydrazyl (DPPH), 2,2′-azino-bis(3-ethylbenzothiazoline-6-sulfonic acid) (ABTS), ferric reducing power, hydrogen peroxide, and hydroxyl radical scavenging assays. The digestive enzyme (α-amylase and α-glucosidase) inhibitory activity was also evaluated. The phytochemical composition of ethyl acetate fraction of *L. cuneata* (Lc-EAF) was studied by UHPLC-QTOF–MS/MS. The effect of Lc-EAF treatments on glucose uptake was studied in insulin resistance HepG2 cells (IR-HepG2). Further, the antidiabetic effect of Lc-EAF in streptozotocin (STZ)-induced diabetic mice were demonstrated. Ethyl acetate, hexane, and methanol fractions of the *L. cuneata* showed notable antioxidant, α-amylase, and α-glucosidase inhibitory properties. Among the fractions, Lc-EAF was found to be the most potent. The Lc-EAF exhibited an IC_{50} of 205.32 ± 23.47 µg/mL and 105.32 ± 13.93 µg/mL for α-amylase and α-glucosidase inhibition, respectively. In addition, 75 µg/mL of Lc-EAF exposure enhanced glucose uptake (68.23%) in IR-HepG2 cells. *In vivo* study indicated that treatment of Lc-EAF (100 mg/kg b.wt) maintained the blood glucose level through reduced insulin level while improving the lipid profile, hepatic, and renal markers. These findings suggest that Lc-EAF could be considered a prominent source for antidiabetic, anti-hyperlipidemic, and anti-ROS potentials.

Keywords *Lespedeza cuneata* · Antioxidant · Antidiabetic · Streptozotocin · ICR mice

Abbreviations

ABTS	2,2′-Azino-bis(3-ethylbenzothiazoline-6-sulfonic acid
ALP	Alkaline phosphatase
ALT	Alanine aminotransferase
ALT	Aspartate aminotransferase
B.wt	Body weight
BUN	Blood urea nitrogen
DM	Diabetes mellitus
DNS	3, 5-Dinitrosalicylic acid
DPPH	1,1-Diphenyl-2-picrylhydrazyl
GAE	Gallic acid equivalents
HDL-C	High-density lipoprotein cholesterol
IP	Intraperitoneal
IR-HepG2	Insulin resistance HepG2 cells
Lc-EAF	Ethyl acetate fractions of *L. cuneata*
Lc-HF	Hexane fractions of *L. cuneata*
Lc-MF	Methanol fractions of *L. cuneata*

Responsible Editor: Mohamed M. Abdel-Daim

Arokia Vijaya Anand Mariadoss and SeonJu Park contributed equally to this work.

✉ Myeong-Hyeon Wang
mhwang@kangwon.ac.kr

[1] Department of Bio-Health Convergence, Kangwon National University, Chuncheon 200-701, Republic of Korea

[2] Department of Orthopaedic Surgery, Dongtan Sacred Heart Hospital, Hallym University College of Medicine, Hwaseong 18450, Republic of Korea

[3] Chuncheon Center, Korea Basic Science Institute (KBSI), Chuncheon 24341, Republic of Korea

LDL-C	Low-density lipoprotein cholesterol
QE	Quercetin equivalents
STZ	Streptozotocin
TPC	Total phenolic content

Introduction

In the present world scenario, around 422 million people are suffering from obesity-related type 2 diabetes mellitus (Sun et al. 2022). According to World Health Organization statistics, by 2030, this number will be almost doubled (Ali et al. 2021). Diabetes mellitus (DM) is one the most severe widespread carbohydrate metabolic disorders, and it is one of the ninth leading causes of death worldwide, predominantly in developed and developing countries, including South Korea (Khan et al. 2020; Magliano et al. 2021). The sudden increase of DM in South Asia is more than 150% between 2000 and 2035. The drastic incidence of DM significantly increased in the last three decades in the South Korean population (13.7%) (Oh et al. 2021). According to the Korean National Health and Nutrition Examination Surveys, the prevalence of diabetes increased from 8.9 to 11.1% in the young Korean population. Ageing, obesity, urbanization, food habits, and socioeconomic status are the common risk factors for DM. Moreover, the age-specific prevalence of diabetes has been recorded worldwide over the last three decades (Mirzaei et al. 2020; Oyewande et al. 2020; Wang et al. 2020).

The current therapeutical systems failed to completely cure metabolic diseases, including DM, due to poor target specificity and less availability of the diabetic drug. While medical researchers have advanced diabetic prevention and treatment, they continue to look for new antidiabetic drugs (Mohan et al. 2020). However, the remarkable accomplishment of synthetic drugs from "bench to bedside" for human use has met restricted success because many of the drugs have significant unfavorable effects. The use of medicinal plants and their phytoconstituents for DM is not just a search for safer alternatives to pharmaceuticals. They can effectively lower blood glucose levels and insulin resistance, decrease diabetic-associated metabolic complications, and improve insulin secretion and the antioxidant system (Vinayagam et al. 2016, 2017). Several research studies proved that phytoconstituents have always guided the search for a clinical trial. Hence, novel dietary phytoconstituents have emerged with natural antioxidants that can be used as antidiabetic compounds (Sun et al. 2020; Wang et al. 2013).

In diabetes conditions, the carbohydrate metabolizing enzymes of α-amylase and α-glucosidase break down the carbohydrate molecule and raise the postprandial glucose level. Prior investigation has implemented that controlling the activity of these two enzymes can lower the risk of developing diabetes and postprandial hyperglycemia (Poovitha and Parani 2016). Several inhibitors of α-amylase and α-glucosidase have been found in medicinal plants. These could be used as an alternative drug that is more effective and has fewer side effects than the synthetic drug that is currently used (Huneif et al. 2022; Tshiyoyo et al. 2022). These enzyme inhibitors are also known as starch blockers because they prevent or delay starch absorption into the body by preventing the hydrolysis of 1,4-glycosidic linkages in starch and other oligosaccharides into simple sugars (Dineshkumar et al. 2010).

Based on this scientific knowledge, the present study is designed to evaluate the antidiabetic effect of the active fraction of *Lespedeza cuneata* through the deactivation of the streptozotocin-induced diabetic model. *Lespedeza cuneata* is a perennial herbaceous shrub belonging to the family of Fabaceae. It is widely distributed in the Korean peninsula, Japan, India, China, Taiwan, Nepal, Vietnam, and Bhutan. It is also cultivated in Australia, North America, South America, and the Caribbean (Lee et al. 2011). The root and leaf parts of *L. cuneata* contain vitamins and minerals. Phytochemical analyses have shown that it has a rich source of flavonoids, pinitols, phenylpropanoids, sterols, tannins, triterpenoids, lignins, etc. Preliminary reports confer anti-inflammatory, anticancer, antioxidant, antimicrobial, antiaging, and hepatoprotective activities (Cho et al. 2009; Kim and Kim 2007, 2010; Lee et al. 2013; Zhang et al. 2016). Besides, the extract of the plant material has a long history in folk medicine to treat severe chronic cough, abscess, asthma, and eye diseases (Lee et al. 2019). Flavonoid compounds isolated from *L. cuneata* have a considerable free radical scavenging activity (Kim et al. 2011). Aqueous extracts of *L. cuneata* have considerably inhibited the diabetic-related enzyme of DPP-IV and α-glucosidase activity (Sharma et al. 2014). Moreover, few studies have focused on the antidiabetic efficacy of the bioactive fraction of *L. cuneata.* Hence, our present study intended to explore the phytochemical profile (total phenolic and flavonoid content) and antioxidant properties (DPPH, ABTS, hydroxyl radical, and ferric reducing power assay) of ethyl acetate fraction of *L. cuneata* and its effect on treating STZ-induced type 2 diabetic ICR mice.

Materials and methods

Chemicals

Streptozotocin (Cat. No. 572201), insulin (Cat. No. I2643), citrate buffer (Cat. No. C2488), sodium carbonate (Cat. No. 222321), sodium nitrate (Cat. No. S5506), sodium hydroxide (Cat. No. 221465), ascorbic acid (Cat. No. PHR1008), aluminum chloride (Cat. No. 8010810500), potassium ferricyanide (Cat. No. 702587), trichloroacetic acid (Cat. No. T6399), EDTA (Cat. No. E9884), potassium acetate (Cat. No. P1190), quercetin (Cat. No. PHR1488), gallic acid (Cat. No. 91215), ABTS

reagent (Cat. No. 10102946001), Folin-Ciocalteu reagent (Cat. No. F9252), and ethanol (Cat. No. 1009831011) were obtained from Sigma Chemical Co. (St. Louis, MO, USA). Methanol (Cat. No. 5558–4410), ethyl acetate (Cat. No. 4016–4410), and n-hexane (Cat. No. 4081–4110) were procured from Daejung Chemicals & Metals Co., Ltd. (South Korea). DMEM (Cat. No. 11965–092), fetal bovine serum (Cat. No. 26140–079), antibiotic solution (Cat. No. 15140–122), phosphate buffer saline (Cat. No. 2219206), and trypsin EDTA (Cat. No. 25200–056) were procured from Gibco Chemicals and Corning (USA). The WST solution (Cat. No. CM-VA1000) was purchased from Mediflab, Seoul, South Korea.

Preparation of plant extracts/active fraction

Dried leaves of *L. cuneata* were purchased from the local market of Chuncheon, South Korea. The taxonomic authentication was done by the professor. According to MH Wang at the Department of Bio-health Convergence, the voucher specimen (KNUH-BMC-2020–006) was deposited in the herbarium of the Department of Biomedical Convergence, Kangwon National University, South Korea. The leaf part of *L. cuneata* was crushed in a grinder. Then, 100 g powdery samples of *L. cuneata* were extracted with 500 mL of methanol three times at room temperature. After 2 days of incubation, the resulting mixture was filtered with Whatman No 1 filter paper, and then, it was concentrated at reduced pressure. Then, 10 g of concentrated methanol crude extract was fractionated using hexane, ethyl acetate, and methanol as solvents. Under the reduced pressure atmosphere in a rotary vacuum evaporator at 40℃, the collected fraction was concentrated. Then, the dried sample was stored at − 20℃ for further analysis.

Estimation of total phenolic and flavonoid content

The total phenolic content (TPC) was determined using the Folin-Ciocalteu reagent and expressed in milligram of gallic acid equivalents (GAE) (Singleton et al. 1999). Briefly, an aliquot of 100 µL of Lc-MF, Lc-HF, and Lc-EAF was mixed with 200 µL of freshly made Folin reagent (1:10 v/v in water) and left at 25 °C for 5 min. Then, 200 µL of sodium bicarbonate (75 g/L) solution was added to the mixture. The mixture was left to sit at 25 °C for 90 min, and the absorbance at 760 nm was measured with a microplate spectrophotometer (SpectraMax® ABS Plus, Molecular Devices, CA, USA). Total flavonoid content was measured by the method described by Zhishen et al. (1999). In 1.5 mL of Eppendorf tube, 50 µL of Lc-MF, Lc-HF, and Lc-EAF, 200 µL of distilled water, 150 µL ethanol (95%), and 10 µL of aluminum chloride were added. Then, 10 µL of sodium acetate was added after 5 min. After thoroughly mixing the solution, the absorbance was calculated at 415 nm and compared to the reagent blank. The same method previously described was used to generate the standard curve using quercetin.

Estimation of antioxidant activity

The method proposed by Zakaria et al. (2008) was used to find the 1,1-diphenyl-2-picrylhydrazyl (DPPH) scavenging efficacy of Lc-MF, Lc-HF, and Lc-EAF. 1×10^4 M methanolic dilution of DPPH was made before the assay. Different concentrations of an equal volume of the test sample (100 µL) and DPPH solution were mixed and kept in the dark at room temperature for 10 min. The absorbance was measured at 517 nm with a UV spectrophotometer (Zakaria et al. 2008). The radical scavenging capacity of ABTS was determined using the method described by Zhou et al. (2013). 100 µL of varying concentrations of Lc-MF, Lc-HF, and Lc-EAF was mixed with 100 µL ABTS radical solution. After 30 min of reaction, the absorbance at 734 nm was measured (Zhou et al. 2013). The hydroxyl radical scavenging activity of the test samples was measured using the previously described method by Halliwell et al. (1987) with minor modifications. The assay mixture consists of deoxyribose (2.8 mM), KH_2PO_4-NaOH buffer, pH 7.4 (0.05 M), FeCl3 (0.1 mM), EDTA (0.1 mM), H_2O_2 (1 mM), and various concentrations of Lc-MF, Lc-HF, and Lc-EAF. After 30 min of incubation at 37 °C, 2 mL of trichloroacetic acid (2.8%w/v) and thiobarbituric acid was added. After that, it was cooled in a water bath for 30 min. A UV–Vis spectrophotometer was used to measure absorbance at 532 nm. The reducing antioxidant power of the sample was determined using the method described by Oyaizu (1986). Briefly, various concentrations of Lc-MF, Lc-HF, and Lc-EAF were mixed with 250 µL of phosphate buffer (0.2 M, pH 6.6) and 250 µL of potassium ferricyanide in 100 µL of distilled water, and it was allowed for 20-min incubation at 50 °C. Then, the solution was then treated with 250 µL of 10% trichloroacetic acid and centrifuged for 10 min at 3000 rpm. The upper layer of the solution was mixed with an equal volume of distilled water (~250 µL), and the solution absorbance at 700 nm against a blank was used to measure the reducing power ability of the test materials. All the assay was repeated three times, and the percentage of absorbance of ABTS, DPPH, hydroxyl radical, and ferric-reducing power assay inhibition was calculated using the following formula:

$$\%\ \text{radical scavenging activity} = \left\{\left(\text{OD}_{\text{control}} - \text{OD}_{\text{sample}}\right)/\text{OD}_{\text{control}}\right\} \times 100;$$

where OD is the absorbance of the samples.

Determination of α-amylase and α-glucosidase inhibition activity

The method of Sudha et al. (2011) was used to assess the α-amylase activity of test samples with some modifications. Simply boiling and stirring 20 mg of starch in 10 mL of 200 mM sodium phosphate buffer (pH 6.9) for 15 min yielded a starch solution (2 mg/mL). The enzyme solution (4 units/mL) was made by combining 0.001 g of α-amylase (Sigma-Aldrich, St.

Louis, MO, USA) with 1.5 mL of the buffer mentioned above. As a color reagent, dinitrosalicylic acid (DNSA) was used. The reaction mixture compressed of 100 µL of varying concentration of Lc-MF, Lc-HF, and Lc-EAF was mixed with 300 µL of starch solution, 20 µL of α-amylase, and 40 µL 2 M sodium hydroxide and incubated at 37 °C for 15 min; then, 40 µL of DNSA was added to this mixture, and the tube was incubated at 85 °C in a water bath. The reaction mixture was removed from the water bath and cooled after 15 min. A microplate spectrophotometer was used to measure the absorbance at 540 nm.

The α-glucosidase inhibitory activity was assessed by the method of Liu et al. (2016). Briefly, 100 µL of varying concentrations of Lc-MF, Lc-HF, and Lc-EAF was mixed with 100 µL α-glucosidase and 125 µL of p-nitrophenyl-α-D-glucopyranoside (3 mM). The test solution was kept at 37 °C for 30 min to start the enzymatic reaction. Subsequently, 500 µL sodium carbonate was added to the solution to arrest the reaction. Using a microplate spectrophotometer, the enzymatic activity was quantified by measuring absorbance at 405 nm. This assay was repeated three times.

Biocompatible nature of *L. cuneata*

The biocompatibility of *L. cuneata* extracts and active fractions was tested using the mouse embryonic fibroblast cell line of NIH3T3. NIH3T3 cells were obtained from the Korean Cell Line Bank, Seoul, Republic of Korea. Cells were grown in DMEM with 10% fetal bovine serum (FBS) and 0.5% antibiotic solution. The cell lines were grown at 37 °C in a humidified atmosphere containing 5% CO_2. After reaching full confluency, the well-matured cells were trypsinized, seeded into a 96-well plate (10×10^{-4} cells/well), and incubated overnight. Then, 10 µL of varying concentrations (10–100 µg/mL) of Lc-EAF was dissolved and placed in culture plates. Afterward, the plates were placed in a humidified CO_2 chamber for overnight incubation. After that, 10 µL of WST solution was added to each well and reared for another 4 h to determine the cytotoxicity. A multi-functional microplate reader was used to record (OD at 450 nm) the biocompatibility of the tested sample. The experiment was repeated three times, and the findings were statistically represented by the mean and standard deviation (Mariadoss et al. 2020).

Screening of *in vitro* antidiabetic assay in HepG2 cells

A glucose uptake assay was conducted in insulin resistance HepG2 (IR-HepG2) cells to establish the antidiabetic activity of the Lc-EAF. IR-HepG2 cells were first generated according to the protocol reported by Saravanakumar et al. (2021). The well-established IR-HepG2 cells (1×10^4 cells/well) were cultured in high glucose DMEM included with FBS (10%) and antibiotic solution (1%) in a 5% CO_2 incubator for 24 h. For the treatment, various concentrations of Lc-EAF (4.68–300 g/mL) were added to cells and reared for 24 h in the abovementioned conditions. Besides, the negative control (untreated HepG2) cells were maintained. After the incubation, the cells, including the culture media, were harvested and centrifuged at 440 × g for 5 min, and the supernatant was used for glucose assay by DNS method. Glucose uptake (%) was estimated using the method described elsewhere (REF).

UHPLC-QTOF–MS/MS analysis

UHPLC-QTOF–MS/MS was used to identify metabolites present in the ethyl acetate fraction of leaf of *L. cuneata*. The test sample was characterized using a UHPLC QTOF–MS/MS (Waters Xevo G2 QTOFMS, included with the UPLC I-Class system) with *m/z* 50–1600 scanning range negative mode of ionization. An Acquity UPLCBEH C18 column of dimensions 50 mm × 2.1 mm × 1.7 µm was employed. The mobile gradient phase comprised H_2O and CH_3CN (each containing 0.1% HCOOH). With a 0.4 mL/min flow rate and a 2 µL injection volume, gradient elution from 10 to 90% CH_3CN was performed. UNIFI 1.8 with an in-house library was used to analyze the data. With the use of reported values from the literature, resolved peaks were further found.

Computational study

Lipinski's rule of five was employed to predict the drug-likeness of the identified compound from UHPLC-QTOF–MS/MS analysis (Lipinski et al. 1997; Lipinski 2004). Lipinski analysis shows the toxicity profile of selected compounds (vanillic acid 4-*O*-glucoside, glucosyringic acid, *trans*-*O*-coumaric acid 2-glucoside, ferulic acid glucoside, roseoside, and isovitexin) was analyzed by a web server-based ADMET-SAR online tool. The parameters of AMES toxicity, carcinogen, acute oral toxicity, and acute rat toxicity were considered for this analysis (Guan et al. 2019). A computer-based PASS program (prediction of spectra for substances) was used to explore the diabetic-associated pharmacological activity of the selected compounds from *L. cuneata.* The prediction scale was based on the probability to be active (P_a) and probability to be inactive (P_i) (Khurana et al. 2011). In addition, in silico molecular docking study was employed to validate the binding efficiency of selected compounds against the diabetic-related target of α-amylase and α-glucosidase. The target molecule of α-amylase (IOSE) and α-glucosidase (3A4A) was retrieved from the RCSB-PDB protein structure. The non-protein, other ligands, and water molecules were removed before the docking analysis. The selected phytocompounds were retrieved from NIH PubChem, and their energy minimalization was performed

by UCSF Chimera software (Ver 1.14). The docking analysis was performed by ArgusLab 4.0.1, and the results were visualized by using BIOVIA discovery studio visualizer V20 and the parameters like binding energy (kcal/mol), and intermolecular energy (kcal/mol) was calculated to select the best-docked compounds (Anand Mariadoss et al. 2018).

In vivo antidiabetic study

Induction of experimental diabetes

Male ICR mice weighing 19–21 g were used for this study. The mice were randomly separated and maintained in cages at 18–22 °C under normal lighting conditions and allowed to access ad libitum water. All procedures were approved by the Kangwon National University Animal Experimental Ethics Committee (Ethical Approval No. 200813; Dt: 23.12.2020). Type 2 diabetes was induced in 12 h fasted rats by successive i.p. injection of STZ (50 mg/kg b.wt) dissolved in cold citrate buffer (0.1 M, pH 4.5) once a day for 5 consecutive days (Rahmati et al. 2015). STZ-injected animals were given a 20% glucose solution to prevent the initial drug-induced hypoglycemia. The presence of diabetes in rats was established 72 h after injection with STZ by measuring increased plasma glucose (using the glucose oxidase assay). The fasting glucose level > 250 mg/dL was selected as diabetic control for the experiment.

Study design

The experimental animals were separated into five groups, with each group consisting of at least six animals, as indicated below. Lc-EAF and metformin were orally given for 28 days.

Group I: normal rats
Group II: diabetic rats
Group III: diabetic + Lc-EAF (100 mg/kg b. wt)
Group IV: diabetic + metformin (50 µg/kg b.wt)
Group V: normal + Lc-EAF (100 mg/kg b. wt)

Detection of biochemical indexes in serum

After the treatment period, the rats were fasted overnight and sacrificed by cervical decapitation. Fasting blood glucose was estimated by a commercially available glucose kit based on the glucose oxidase method. Serum samples were collected and used for biochemical analysis. The levels of glucose, triglycerides, total cholesterol, low-density lipoprotein cholesterol (LDL-C), high-density lipoprotein cholesterol (HDL-C), alanine aminotransferase (ALT), alkaline phosphatase (ALP), aspartate aminotransferase (ALT), creatinine, and blood urea nitrogen (BUN) content were measured by colorimetric method. Before sacrifice, the animals were allowed to overnight fasting, and intramuscular (IM) injection was ketamine/xylazine (90/10 mg kg^{-1}) and was utilized as an anesthetic agent. The liver, pancreas, and kidney sections were carefully dissected and fixed with 10% buffer formaldehyde solution for 24 h before paraffin embedding. Hematoxylin and eosin (H&E) staining was performed on the paraffin-embedded tissue sample (5 µm), and the stained sections were examined using optical microscopy.

Statistical analysis

One-way analysis of variance was used to evaluate group comparisons, followed by Duncan's multiple range test. IBM SPSS 20 was used for the statistical analysis, and all data are represented as mean ± standard deviation. p value of < 0.05 was considered statistically significant.

Results and discussion

Extraction yield, total phenolic, and flavonoid content

The yields of methanol, hexane, and ethyl acetate fractions of the *L. cuneata* are shown in Table 1. Herein, a different solvent system was selected for the partition of *L. cuneata*. This different solvent system has a prime role in influencing the extraction yield and the quantity of the phytoconstituents. In particular, the ethyl acetate fraction has the maximum extraction yield of 5.59 ± 2.01 mg followed by methanol (2.67 ± 0.98 mg) and hexane (1.81 ± 0.53 mg). It shows the ethyl acetate fraction was considered a suitable choice for the optimum extract yields from the leaf part of *L. cuneata*. In addition, total phenolic and flavonoid contents were measured by the standard spectroscopic method (Table 1). It revealed that the total phenolic and flavonoid contents were significantly ($p < 0.05$) higher in Lc-EAF than in Lc-HF and Lc-MF. Comparatively, Lc-EAF has a higher amount of total phenolic (395.54 ± 5.04 mg/g extract) and flavonoid content (209.63 ± 0.63 mg/g extract). Previous studies also revealed that *L. cuneata* has a higher amount of flavonoid content. Especially the ethyl acetate fraction has a higher amount of phenolic and flavonoid contents due to its polarity nature (Yoo et al. 2015; Zhang et al. 2016). Our results endorsed these findings. In line with the previous works, the present study shows a higher yield of polyhydroxy compounds, glycones, and other organic compounds from the ethyl acetate fraction due to their polar nature (Kifayatullah et al. 2015). These substances are responsible for various pharmacological properties including antioxidant, antidiabetic, antiviral,

Table 1 Extraction yield and total phenolic content and total flavonoid content fractions from *Lespedeza cuneata*

Particulars	Lc-MF	Lc-HF	Lc-EAF
Extraction yield (mg)	2.67 ± 0.98^{b}	1.81 ± 0.53^{a}	5.59 ± 2.06^{c}
Total phenol content (gallic acid equivalent (GAE) mg/g of extract)	46.33 ± 4.97^{b}	39.62 ± 0.32^{a}	359.54 ± 5.04^{c}
Total flavonoid content (quercetin equivalent (QE) mg/g of extract)	32.73 ± 0.31^{a}	67.97 ± 1.85^{b}	209.63 ± 0.63^{c}

The different superscript letters in the same column of the different fractions show the significant difference by Duncan's multiple range test ($p < 0.05$)

anticancer, and anti-inflammatory activities (Cho et al. 2009; Kim and Kim 2010; Lee et al. 2013; Yoo et al. 2015).

Antioxidants and free radical scavenging activity

A variety of in vitro studies assessed the antioxidant activity of the plant material. DPPH, ABTS, hydrogen peroxide scavenging, hydroxyl radical scavenging, and ferric reducing power are the most regularly used methods. Based on this, the free radical and antioxidant scavenging abilities of the active fraction of the *L. cuneata* associated with DPPH, ABTS, hydroxyl radical, and reducing power assay were studied (Table 2). In the ABTS assay, the IC_{50} value of the Lc-EAF fraction was 58.32 ± 4.21 µg/mL, whereas it was 149.86 ± 10.73 µg/mL and 237.23 ± 19.35 µg/mL, respectively, for Lc-HF and Lc-MF. Likewise, the Lc-EAF fraction (IC_{50} value of 99.54 ± 4.43 µg/mL) showed dose-dependent inhibiting DPPH radical scavenging activity. Thus, in decreasing order, the radical scavenging activity of the *L. cuneata* fraction was Lc-EAF > Lc-HE > Lc-MF. It showed that the ethyl acetate fraction is more active than other fractions ($p < 0.05$). These observations suggest a close link between the phytochemical content and antioxidant activity, such as the radical scavenging effect (DPPH and ABTS assays) (Fernandes de Oliveira et al. 2012). Similarly, dose-dependent hydroxyl radical scavenging activity was observed in our study. The IC_{50} values for the hydroxyl radical scavenging activity by Lc-EAF, Lc-HF, and Lc-MF were 103.16 ± 7.34 µg/mL, 198.44 ± 6.11 µg/mL, and 452.95 ± 19.84 µg/mL, respectively. Similarly, the IC_{50} values for the ferric-reducing power activity by Lc-EAF, Lc-HF, and Lc-MF were 254.37 ± 35.52 µg/mL, 505.81 ± 24.91 µg/mL, and 952.62 ± 15.67 µg/mL. At the highest 1000 µg/mL concentration, Lc-EAF, Lc-HF, and Lc-MF showed considerable antioxidant activity. These results revealed that the antioxidant and free radical scavenging potentials of *L. cuneata* increase with increasing concentrations.

Table 2 Half-maximal inhibitory concentration (IC_{50}) of antioxidants (ABTS, DPPH radical), α-amylase, and α-glucosidase inhibitory activity of different fractions of *Lespedeza cuneata*

Particulars	Lc-MF (µg/mL)	Lc-HF (µg/mL)	Lc-EAF(µg/mL)
ABTS	237.23 ± 19.35^{c}	149.86 ± 10.73^{b}	58.32 ± 4.21^{a}
DPPH	395.73 ± 42.97^{c}	263.62 ± 18.42^{b}	99.54 ± 4.43^{a}
Hydroxyl radical	452.95 ± 19.84^{c}	198.44 ± 6.11^{b}	103.16 ± 7.34^{a}
Reducing power	952.62 ± 15.67^{c}	505.81 ± 24.91^{b}	254.37 ± 35.52^{a}
α-Amylase	682.23 ± 30.86^{c}	407.85 ± 25.54^{b}	205.32 ± 23.47^{a}
α-Glucosidase	403.52 ± 20.17^{c}	286.80 ± 18.86^{b}	105.32 ± 13.93^{a}

The different superscript letters in the same column of the different fractions show the significant difference by Duncan's multiple range test ($p < 0.05$)

α-*Amylase and α-glucosidase inhibition assay*

The in vitro α-amylase and α-glucosidase inhibition assay was performed to explore the inhibitory effect of *L. cuneata*. The results are presented in Table 2. The inhibitory action of the active fraction of *L. cuneata* against α-amylase was dose-dependent from 10 to 1000 µg/mL concentrations. Lc-EAF showed the lowest value, which indicates a high inhibitory activity towards the enzyme. The IC_{50} values for the α-amylase inhibitory activity of Lc-EAF, Lc-HF, and Lc-MF were 205.32 ± 23.47 µg/mL, 407.85 ± 25.54 µg/mL, and 682.23 ± 30.86 µg/mL, respectively. Likewise, the IC_{50} value for the α-glucosidase inhibitory activity of Lc-EAF, Lc-HF, and Lc-MF was 105.32 ± 13.93 µg/mL, 286.80 ± 18.86 µg/mL, and 403.52 ± 20.17 µg/mL, respectively. From the results, it is clear that the phenolic-enriched ethyl acetate fraction of *L. cuneata* was much more effective in inhibiting the activity of α-amylase and α-glucosidase. Consequently, it might be an effective strategy to control or treat DM (Honda and Hara 1993). Other results were broadly in line with previous works (Rohn et al. 2002; Unuofin et al. 2017).

Biocompatibility analysis

To verify the biocompatibility nature of the Lc-EAF, we examined the WST-based cytotoxicity assay in a non-cancerous cell line of NIH3T3 cells. The NIH3T3 cells were subjected to an increasing concentration of Lc-EAF, and the cell viability was monitored for 24 h of incubation. The results revealed that Lc-EAF has a lower cytotoxic effect on NIH3T3 cells, i.e., 1.97 ± 0.87, 3.19 ± 0.46, 6.60 ± 0.18, 8.22 ± 0.47, 9.49 ± 0.69, 10.17 ± 0.56, and 14.85 ± 1.23 µg/mL at a concentration of 4.68, 9.37, 18.75, 37.5, 75, 150, and 300 µg/mL. From these findings, it could be suggested that Lc-EAF does not have any toxic compounds (Fig. 1a).

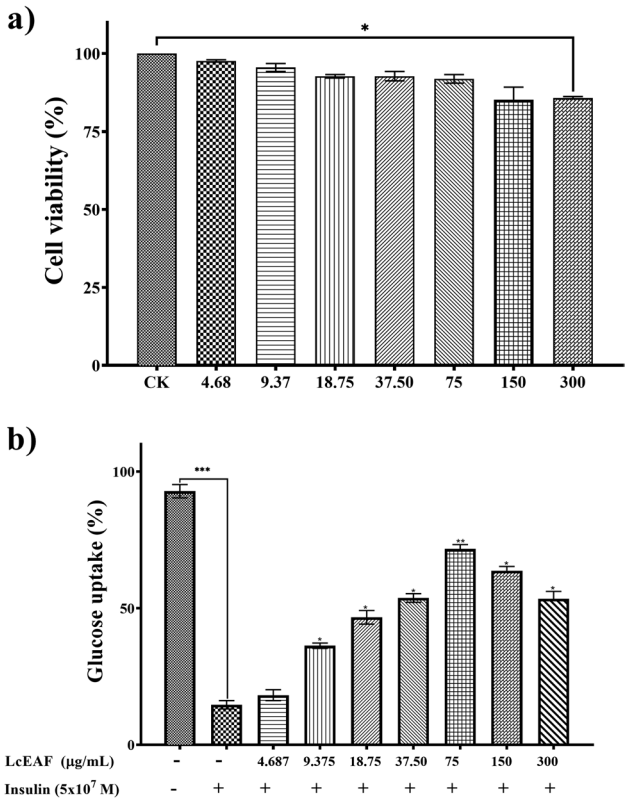

Fig. 1 The biocompatibility nature of Lc-EAF was tested against the non-cancerous cell line of NIH3T3 using WST based cytotoxicity assay (**a**). Lc-EAF stimulates the action of glucose uptake in insulin-resistant HepG2 cells (**b**). The results are presented as mean ± SEM of three different experiments. ***$p < 0.001$, **$p < 0.01$, and *$p < 0.05$ vs. control

Many other studies revealed that most plant-based phytocompounds have biocompatible, non-toxic effects and immensely enhance cell viability. For instance, our previous studies reported that the active fraction of *Helianthus tuberosus* considerably enhances the cell viability of non-cancerous cells (Mariadoss et al. 2021). The fermented and non-fermented extracts of *L. cuneata* exposure surmised the Hs68 (human dermal fibroblast cells) viability, which does not significantly differ from the untreated cells. In the same trend, Park et al. (2020) revealed that the aqueous extracts of *A. manihot* increase cell proliferation.

Glucose uptake in IR-HepG2 cells

The liver is a vital metabolic organ of the body accountable for the normal metabolic pathway. The imbalance in liver metabolism, including glucose and lipid homeostasis, leads to diabetes mellitus through insulin resistance (IR). There is a need for the development of a reliable IR hepatocyte model to study the molecular mechanism of diabetic treatment. (Röder et al. 2016). Based on this, the liver cancer cell line of HepG2 was ideally used to examine IR because the hepatic cells have similar morphological and biochemical features (Donato et al. 2015). Several studies also endorsed this model. We developed IR-HepG2 using a culture media containing high glucose medium and 5×10^{-7} M of insulin, and these established cells were used for this study. Our results explored that the glucose uptake in the IR cells was much lower than in the control cells ($p < 0.001$). Compared to the IR cell, the glucose absorption was significantly boosted after treatment with Lc-EAF in a dose-dependent manner ($p < 0.05$). Among the tested concentration, 75 µg/mL of Lc-EAF showed about 68.23% of glucose uptake. On the contrary, the uptake levels were considerably lower for the concentrations of 150 and 300 µg/mL (Fig. 1b). However, in line with the findings of Nomura et al. (2008), it can be suggested that the bioactive compounds, including quercetin, kaempferol, luteolin, and apigenin, can suppress the IR signaling pathway through the activation of the AKT pathway and inhibition of insulin phosphorylation (Nomura et al. 2008).

UHPLC-QTOF–MS/MS analysis

The Lc-EA fraction was shown to have the most potent radical scavenging ability and intriguing antidiabetic properties. It could be owing to the enrichment of bioactive compounds. As a result, the Lc-EA fraction was used for the UPLC-QTOF-MS/MS analysis. The findings are presented with tentatively identified phytocompound along with formula, RT (min), $[M-H]^-$, *m/z*, response, mass error (ppm), and fragmentation (*m/z*) (Fig. 2 and Table 3). The identified phytocompounds were classified into four groups: flavonoids, phenolics, lignans, and triterpenoids. From the Lc-EAF, 28 compounds were identified by UPLC-QTOF-MS/MS, including seven phenolics (vanillic acid 4-*O*-glucoside, glucosyringic acid, *trans*-*O*-coumaric acid, ferulic acid glucoside, cuneataside A, cuneataside D, and roseoside), sixteen flavonoids (luteolin di-*C*-hexose, taxifolin *O*-glucopyranoside, isorhamnetin-3-*O*rutinoside, apigenin *C*-pentosyl-*C*-hexoside, apigenin di-*C*-pentose, apigenin *C*-hexoside-*O*-pentoside, apigenin di-*C*-hexose, apigenin *O*-hexose (Iso) orientin, quercetin-*O*-rhamnose-*O*-glucoside, (Iso) vitexin, kaempferol-3-glucuronide, nicotiflorin, quercetin-3-*O*glucopyranoside, and luteolin *O*-rutinoside). The bioactive organic fraction of Lc-EAF also contains lignan glycosides of isolariciresinol 9′-*O*-glucoside and secoisolariciresinol-4-*O*-glucopyranoside and the saponin triterpene glycoside. Some of the identified phytocompounds, glucosyringic acid, vanillic acid 4-*O*-glucoside, ferulic acid glucoside *trans*-*O*-coumaric acid 2-glucoside along with the other phenolic compounds, showed significant therapeutic activities including antidiabetic activity (Shahidi and Yeo, 2018). The next category of flavonoids includes luteolin di-*C*-hexose, taxifolin, isorhamnetin-3-*O*-rutinoside, (Iso) orientin,

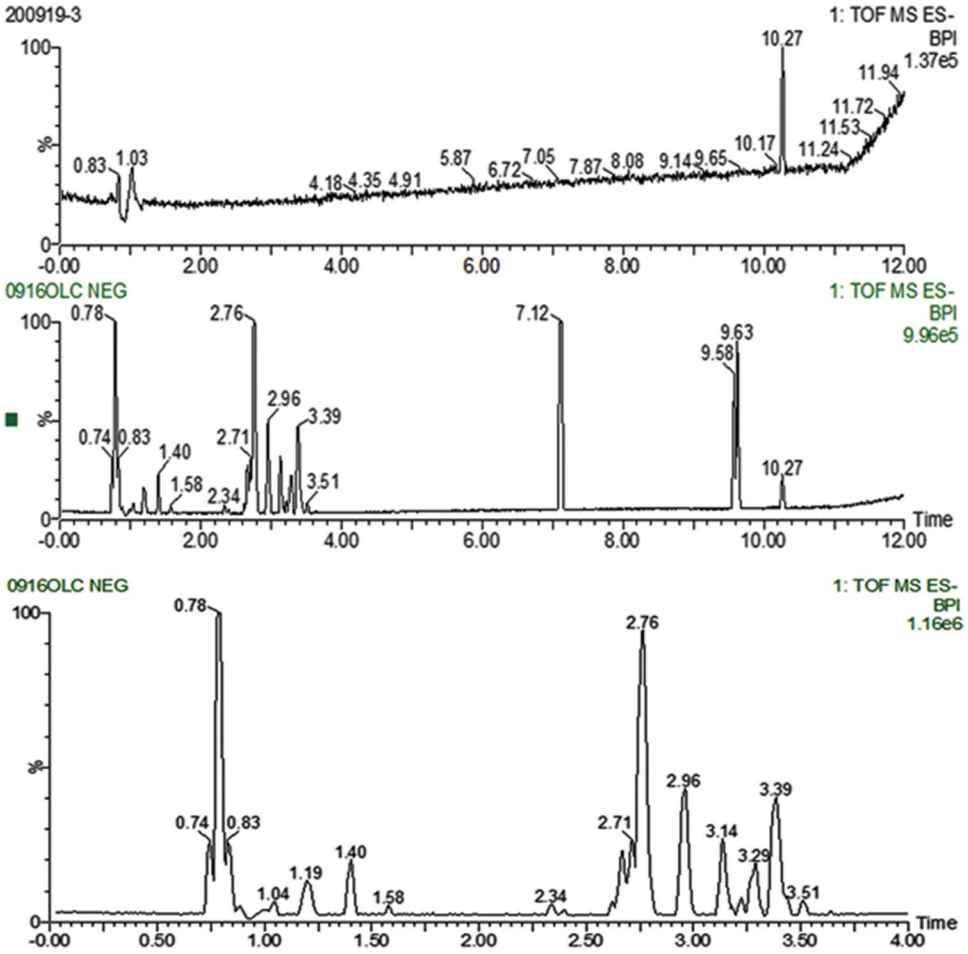

Fig. 2 UHPLC-QTOF–MS/MS analysis of Lc-EAF

quercetin-*O*-rhamnose-*O*-glucoside, (Iso) vitexin, nicotiflorin, kaempferol-3-glucuronide, quercetin-3-*O*-glucopyranoside, and luteolin *O*-rutinoside, which have remarkable antidiabetic, antimicrobial, antimutagenic, and anticancer activities (Kumar and Pandey 2013, Middleton et al. 2000). In addition, there are four apigenin derivatives abundantly present in the Lc-EAF. It is well known that flavonoid-based phytocompounds have significant antidiabetic activity in several types of cell lines and experimental animals (Malik et al. 2017; Qin et al. 2016).

Computational study

Lipinski's rule was adopted to explore the drug-likeness properties of the isolated compounds from Lc-EAF using a web tool of SwissADME. Also, ADMET-SAR online server predicted the toxicological properties of the selected compounds (Sup. Tables 1 and 2). The analysis revealed that the selected compounds (vanillic acid 4-*O*-glucoside, glucosyringic acid, *trans*-*O*-coumaric acid 2-glucoside, ferulic acid glucoside, roseoside, and isovitexin) are non-carcinogenic and had low rat toxicity and acute oral toxicity values. However, the phytocompounds *trans*-*O*-coumaric acid 2-glucoside and ferulic acid glucoside showed AMES toxicity. Besides, the selected compounds also underwent the PASS online tool test to screen the diabetic-related activities, and the potential compounds displayed a higher P_a value than P_i (Sup. Table 3). In silico docking, the analysis showed that selected phytocompounds act as a potential inhibitor of α-amylase and α-glucosidase. The interaction poses of vanillic acid 4-*O*-glucoside, glucosyringic acid, *trans*-*O*-coumaric acid 2-glucoside, ferulic acid glucoside, roseoside, and isovitexin with the target protein of α-amylase and α-glucosidase are shown in Fig. 3 and Fig. 4, respectively, and the relevant data are collected in Table 4. Our studies revealed that among the tested compounds, *trans*-*O*-coumaric acid 2-glucoside binds with the α-amylase with higher affinity with a docking score of − 9.99503 kcal/mol. It directly binds to the amino acid residues of Gly304, Arg 346, Thr 314, Asp 317, and Arg 267 in IOSE. Besides, glucosyringic acid has a docking score of − 8.59 kcal/mol with 3A4A (α-glucosidase). It was directly bound with the amino acid residues of Leu 434, Trp 402, Lys 400, Tyr 407, and Asn 401 in 3A4A through hydrogen bonding. The docking results of other tested phytocompounds are shown in Fig. 3 and Table 4.

Table 3 Quantitative phytocompounds from the ethyl acetate fraction of *Lespedeza cuneate* by UPLC-QTOF-MS/MS analysis

RT (min)	Tentative identification	Formula	*m/z* (M-H)-	Mass error (ppm)	Response	Fragmentation (*m/z*)	Reference
1.19	Vanillic acid 4-*O*-glucoside	C14H18O9	329.0881	1.0	6729	167.0349	Virgen-Ortíz et al. (2016)
1.36	Glucosyringic acid	C15H20O10	359.0985	0.4	3956	166.0001, 197.0458	Kaszás et al. (2020)
1.48	Hydroxycinnamic acid *O*-glucoside	C15H18O8	325.0926	1.2	2046	119.0513, 163.0402	Virgen-Ortíz et al. (2016)
1.67	Ferulic acid glucoside	C16H20O9	355.1040	1.6	3589	134.0377, 193.0503	Piraud et al. (2003)
1.95	Luteolin di-*C*-hexose	C27H30O16	609.1458	−0.5	17,518	369.0615, 489.1041	Zhang et al. (2017)
2.03	Taxifolin *O*-glucopyranoside	C21H22O12	465.1044	1.1	2653	285.0407, 303.498	Bianco et al. (2001)
2.45	Isolariciresinol 9'-*O*-glucoside	C26H34O11	521.2022	−1.1	2338	329.1047, 344.1263, 359.1496	Zhou et al. (2016)
2.63	Luteolin *C*-pentosyl-*C*-hexoside	C26H28O15	579.1356	0.0	54,263	429.0828, 459.0937	Ruan et al. (2019)
2.67	Unknown	C19H30O8	385.1865	−0.4	209207	-	-
2.88	Apigenin *C*-pentosyl-*C*-hexoside	C26H28O14	563.1404	−0.4	16373	353.0666, 473.1090	Ruan et al. (2019)
2.96	(Iso)Orientin	C21H20O11	447.0932	−0.2	407537	284.0323, 297.0403, 327.0509, 357.0614	Karar and Kuhnert (2015)
3.14	Apigenin di-*C*-pentose	C25H26O13	533.1302	0.3	219194	353.0666, 383.0771, 443.0986	Geng et al. (2016)
3.18	Apigenin *C*-hexoside-*O*-pentoside	C26H28O14	563.1407	0.1	41366	293.0454, 413.0880	Bender et al. (2018)
3.22	Quercetin-*O*-rhamnose-*O*-glucoside	C27H30O16	609.1462	0.1	60370	300.0274	Li et al. (2014)
3.39	(Iso)Vitexin	C21H20O10	431.0985	0.4	392599	311.0560, 341.0666	Karar and Kuhnert (2015)
3.43	Kaempferol-3-glucuronide	C21H20O12	463.0884	0.4	37174	285.0404	Kaszás et al. (2020)
3.44	Nicotiflorin	C27H30O15	593.1515	0.6	67825	285.0404	Bianco et al. (2001)
3.52	Quercetin-3-*O*-glucopyranoside	C21H20O12	463.0884	0.3	65361	300.0276	Virgen-Ortíz et al. (2016)
3.62	Apigenin di-*C*-hexose	C27H30O15	593.1522	1.7	3318	353.0674, 473.1096	Zhang et al. (2017)
3.74	Apigenin *O*-hexose	C21H20O10	431.0985	0.5	9142	269.0449	Piraud et al. (2003)
3.82	Luteolin *O*-rutinoside	C27H30O15	593.1516	0.7	4457	285.0399	Bianco et al. (2001)
3.95	Isorhamnetin-3-*O*-rutinoside	C28H32O16	623.1611	−1.1	2156	300.0271, 315.0510	Zhang et al. (2017)
3.99	Secoisolariciresinol-4-*O*-glucopyranoside	C26H36O11	523.2187	0.3	15311	346.1426, 361.1656	Jeong et al. (2020)
4.92	Cuneataside A	C31H36O15	647.1980	−0.2	3334	145.0298, 163.0403, 501.1612	Zhou et al. (2016)
5.87	Cuneataside D	C28H34O13	577.1928	0.2	3078	145.0300, 163.0404, 341.1051, 415.1418	Zhou et al. (2016)
7.11	Unknown	C41H56O7	659.3939	−1.6	1659646	599.3732	-
9.58	Triterpene glycoside	C47H76O17	911.5005	−0.5	559477		-
9.63	Triterpene glycoside	C49H80O20	987.5159	−1.2	594216		-

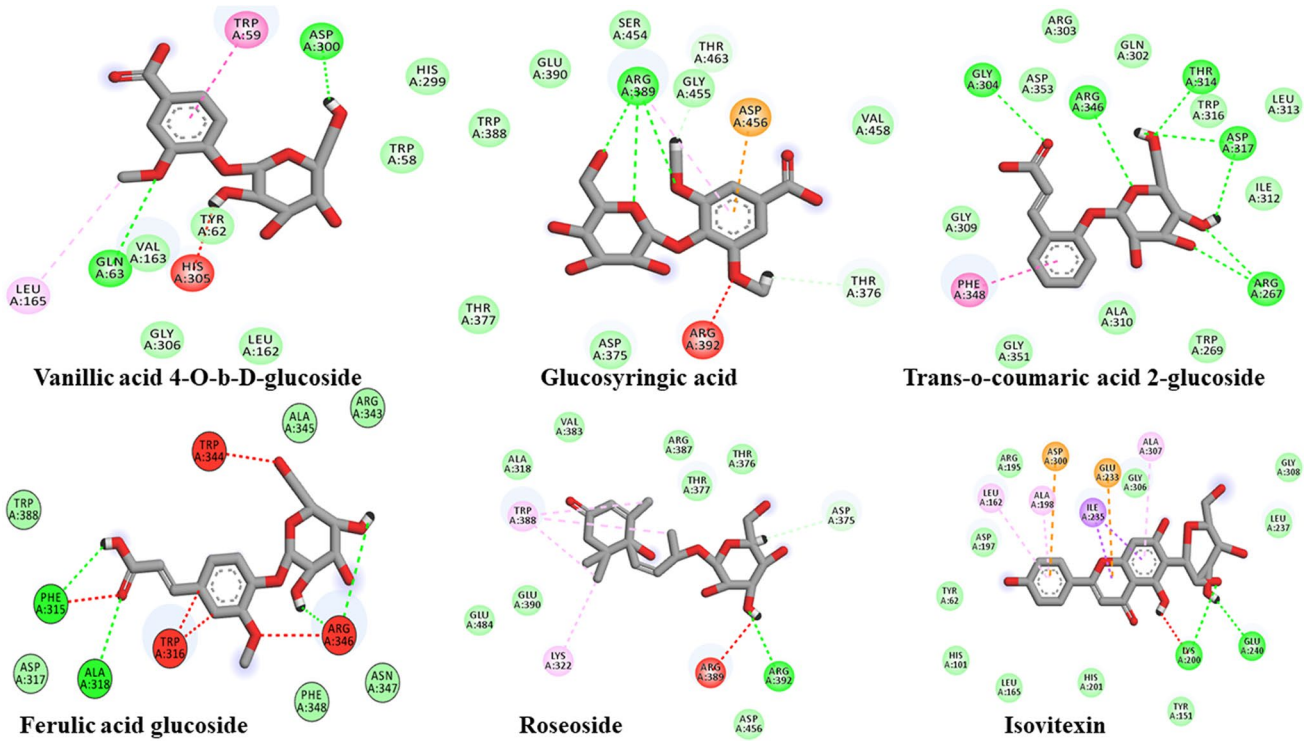

Fig. 3 Molecular docking analysis of selected phytocompound from Lc-EAF against the antidiabetic target of α-amylase

Antidiabetic activity of Lc-EAF in ICR mice

Diabetes is characterized by high blood glucose levels,

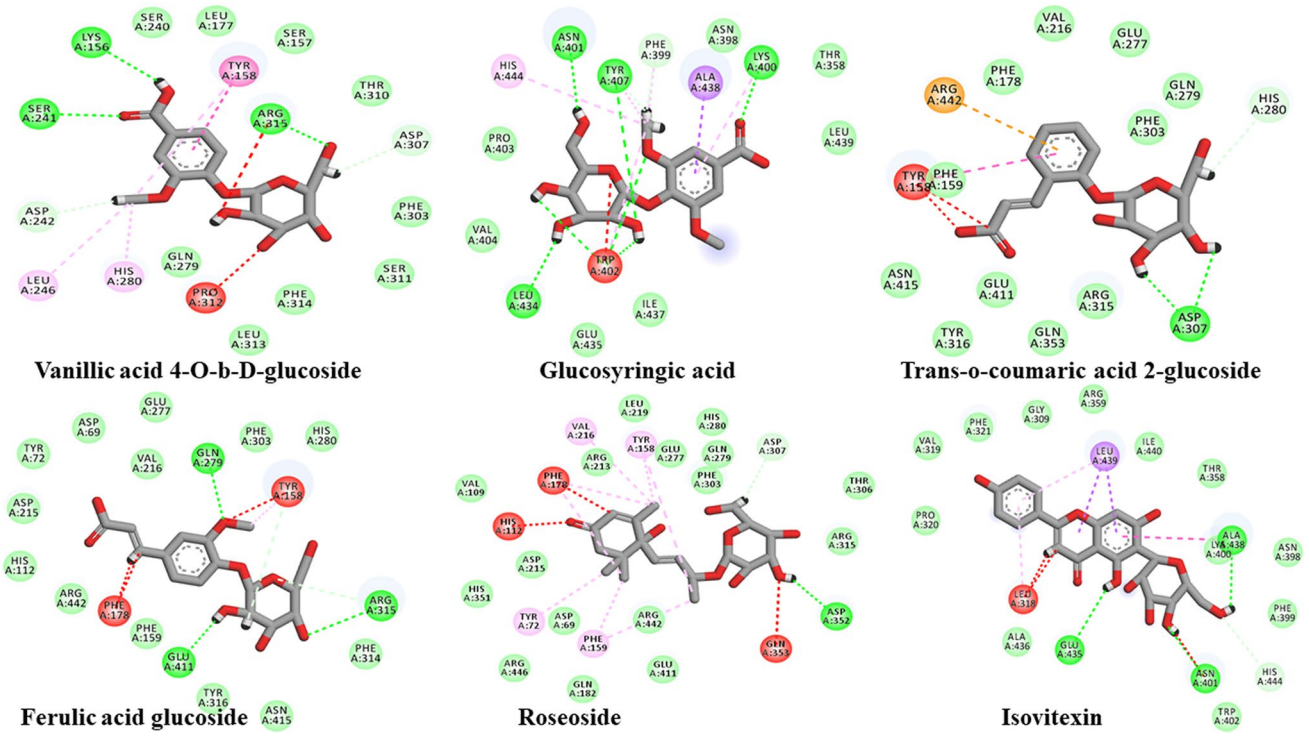

Fig. 4 Molecular docking analysis of selected phytocompound from Lc-EAF against the antidiabetic target of α-glucosidase

Table 4 Molecular docking analysis of selected phytocompound from Lc-EAF against the antidiabetic target of α-amylase and α-glucosidase

Phytocompound	Docking score (kcal/Mol)	Interactive residues of H-bond	Other interactive residues
α-Amylase			
Vanillic acid 4-*O*-glucoside	−8.04	2 (Gln 63, Asp 300)	His 299, Trp 58, Leu 162, Gly 306, Leu 165, Val 163, Tyr 62, Gly 306, Leu 162
Glucosyringic acid	−8.33	3 (Arg 389)	Gly 455, Thr 463, Thr 376, Asp 456, Arg 392, Asp 375, Thr 377, TRP 388, Glu 390, Ser 390, Val 458
trans-*O*-Coumaric acid 2-glucoside	−9.99	7 (Gly304, Arg 346, Thr 314, Asp 317, Arg 267)	Phe 348, Gly 309, Asp 353, Arg 303, Gln 302, Trp 316, Leu 313, Ile 312, Trp 269, Ala 310, Gly 351
Ferulic acid glucoside	−9.03	4 (Phe 315, Ala 318, Arg 346)	Asp 317, Trp 388, Trp 344, Ala 345, Arg 343, Asn 347, Phe 348, Trp 316
Roseoside	−8.72	1 (Arg 392)	Arg 389, Asp 456, Lys 322, TRP 388, Glu 484, Glu 390, Ala 318, Val 318, Arg 387,Thr 376, Thr 377, Asp 375
Isovitexin	−8.08	2 (Lys 200, Glu 240)	Leu 162, Ala 198, Asp 300, Ile 235, Glu 233, Gly 306, Ala 307, Gly 308, Leu 237, Tyr 151, His 201, Leu 165, His 101, Tyr 62, Asp 197, Arg 195
α-Glucosidase			
Vanillic acid 4-*O*-glucoside	−8.51	3 (Ser 241, Lys 156, Arg 315)	Tyr 158, Asp 307, Pro 312, His 280, Leu 246, Tyr 158, Asp 242, Ser 240, Leu 177, Ser 157, Thr 310, Phe 303, Ser 311, Phe 314, Leu 313, Gln 279
Glucosyringic acid	−8.59	7 (Leu 434, Trp 402, Tyr 407, Asn 401, Lys 400)	Phe 399, Ala 438, Asn 398, Thr 358, Lu 439, Ile 437, Glu 435, Val 404, Pro 403, His 444
trans-*O*-Coumaric acid 2-glucoside	−9.03	2 (Asp 307)	Tyr 158, Phe 159, Arg 442, His 280, Arg 315, Gln 353, Glu 411, Tyr 316, Asn 415, Phe 178, Val 216, Glu 277, Phe 303, Gln 279
Ferulic acid glucoside	−9.40	3 (Gln 279, Arg 315, Glu 411)	Phe 178, Tyr 158, Phe 314, Asn 415,Tyr 316, Phe 159, Arg 442, His 112, Asp 215, Tyr 72, Asp 69, Val 216, Glu 277, Phe 303, His 280, Phe 314, Asn 415, Tyr 316
Roseoside	−9.33	1 (Asp 352)	Gln 353, His 112, Phe 178, Val 216, Tyr 158, Arg 442, Glu 411, Gln 182, Phe 159, AsP 69, Tyr 72, Arg 446, His 351, Asp 215, Val 109, Arg 213, Leuy 219, Glu 277, His 280, Gln 279, Phe 303, Asp 307, Thr 306, Arg 315
Isovitexin	−6.86	3 (Glu 435, Asn 401, Ala 438)	Lys 400, Leu 439, Leu 318, Trp 402, His 444, Phe 399, Asn 398, Thr 358, Ile 440, Arg 359, Gly 309, Phe 321, Val 319, Pro 320

excessive urination, excessive thirst, and weight loss despite increased appetite. Table 5 shows the blood glucose level, body weight, kidney, and liver weight of the experimental animals in each group. In the end, the STZ alone-treated mice showed an increased blood glucose level (387.21 ± 9.34 mg/dL). These levels were significantly reduced in diabetic ICR mice after Lc-EAF treatment. Besides, the body and organ weight were significantly decreased in diabetic animals compared to non-treated control mice. The STZ alone-treated mice lost body weight (−3.12 ± 0.93), and the relative liver weight was found to be 4.17 ± 0.81. These levels were significantly lower in the rest of the other experimental groups. The Lc-EAF treatment has significantly balanced the body weight and organ weight in diabetic mice. We also monitored the caloric intake and water intake of the animals daily. A significant reduction in body weight was seen in STZ-induced diabetic mice compared to the control group (Saadane et al. 2020). Lack of insulin may account for this, as it causes glucose to be unable to enter the cell, thereby increasing the

Table 5 Changes in the blood glucose, body weight, and organ weight of the control and Lc-EAF-treated experimental mice. The different superscript letters in the same column of the different group show the significant difference by Duncan's multiple range test ($p < 0.05$)

Group	Blood glucose		Body weight			Liver weight (g)	Kidney weight (g)	Relative liver weight (g/100 g b.wt)
	Initial (mg/dL)	Final (mg/dL)	Initial (g)	Final (g)	Weight gain (g)			
Control	92.23 ± 5.16^{a}	97.14 ± 4.87^{a}	30.92 ± 1.79^{a}	$32.46 \pm 1.02b$	2.26 ± 0.79^{b}	1.63 ± 0.02^{d}	0.64 ± 0.02^{b}	5.02 ± 0.12^{d}
STZ	295.54 ± 15.79^{c}	403.21 ± 17.34^{d}	32.49 ± 1.12^{b}	29.19 ± 1.87^{a}	-3.12 ± 0.93^{d}	1.22 ± 0.27^{a}	0.57 ± 0.05^{a}	4.17 ± 0.81^{b}
STZ + Lc-EAF	261.94 ± 18.83^{b}	130.25 ± 12.11^{c}	32.22 ± 1.32^{b}	34.55 ± 1.32^{b}	2.33 ± 0.74^{c}	1.40 ± 0.04^{b}	0.58 ± 0.03^{a}	4.05 ± 0.18^{a}
STZ + metformin	$269.04 \pm 16.58^{b,c}$	116.97 ± 7.48^{b}	34.17 ± 2.03^{b}	36.54 ± 1.27^{b}	2.47 ± 1.68^{c}	1.55 ± 0.07^{c}	0.56 ± 0.04^{a}	4.24 ± 0.24^{b}
Lc-EAF alone	94.56 ± 6.48^{a}	102.48 ± 5.28^{a}	35.80 ± 2.00^{b}	37.25 ± 2.15^{c}	1.75 ± 0.40^{a}	1.61 ± 0.08^{d}	0.65 ± 0.03^{b}	4.86 ± 0.30^{c}

Table 6 Influence of Lc-EAF in plasma lipid profile of control and experimental mice. The different superscript letters in the same column of the different group show the significant difference by Duncan's multiple range test ($p < 0.05$)

Group	Total cholesterol (mg/dL)	Triglycerides (mg/dL)	HDL (mg/dL)	LDL (mg/dL)	Total cholesterol/HDL-C ratio	LDL-C/HDL-C ratio
Control	76.00 ± 3.48^{a}	65.08 ± 4.48^{a}	36.97 ± 3.48^{c}	23.38 ± 3.31^{a}	2.05 ± 0.04^{a}	0.63 ± 0.06^{a}
STZ	129.05 ± 8.65^{d}	116.94 ± 5.42^{d}	24.09 ± 1.29^{a}	55.14 ± 3.10^{d}	6.14 ± 0.43^{c}	2.71 ± 0.03^{d}
STZ + Lc-EAF	109.66 ± 7.84^{c}	87.99 ± 5.25^{c}	35.56 ± 2.70^{c}	34.93 ± 6.20^{c}	3.08 ± 0.07^{b}	0.98 ± 0.02^{c}
STZ + metformin	92.61 ± 4.83^{b}	80.76 ± 7.23^{b}	30.86 ± 2.67^{b}	27.46 ± 4.24^{b}	3.01 ± 0.02^{b}	0.88 ± 0.03^{b}
Lc-EAF alone	72.39 ± 2.16^{a}	63.39 ± 2.84^{a}	34.95 ± 2.20^{c}	24.62 ± 3.10^{a}	2.07 ± 0.01^{a}	0.70 ± 0.04^{a}

percentage of sugar in the blood. To eliminate excess sugar, the body attempts to clear itself sugar through excretion in the urine (Cantley and Ashcroft 2015). An increase in urine production will lead to dehydration and weight loss. While hyperglycemic STZ-induced ICR mice were found to have significantly increased food and water intake, the increased food and water intake of these mice is likely due to a reduction in glucose utilization and significant loss of glucose in the urine, resulting in a stimulus to eat and drink (data are not shown). The improvement in polyphagia, polydipsia, and preventing weight loss seen in STZ-induced ICR mice was strongly correlated with improved metabolic status and intestinal absorption in Lc-EAF-supplemented mice. The low dose of STZ (50 mg/kg b.wt) causes pancreatic β-cells to be destroyed in rats, which results in insufficient insulin secretion. This model mimics the clinical condition of type 2 diabetes. The level of plasma glucose increased while the level of insulin decreased (Table 5). The ability of Lc-EAF to stimulate insulin secretion from the remnant β-cells and increase glucose utilization by the tissues is responsible for reducing fasting plasma glucose levels in diabetic rats. These findings are supported by increased insulin secretion in diabetic rats on Lc-EAF treatment.

The current study has shown that elevated levels of hepatic lipids are commonly found in people with diabetes, which can serve as a valuable risk factor for cardiovascular problems. Additionally, increased concentrations of fatty acids also promote the oxidation of fatty acids, resulting in more acetyl CoA and cholesterol, which cause hypercholesterolemia (Martín-Timón et al. 2014). As indicated by increased plasma cholesterol, TGs, LDL, and diminished HDL, dyslipidemia was detected in STZ-induced ICR mice in the current study. Thus, we suggest that Lc-EAF could treat hyperlipidemia by reducing cholesterol, TGs, and LDL and increasing HDL levels in diabetic mice (Table 6). Because of an increase in insulin secretion, there was a reduction in cholesterol synthesis, which accounts for the anti-hyperlipidemic effect (Srinivasan and Pari 2013). In addition, Lc-EAF is thought to lower cholesterol levels by inhibiting cholesterol uptake from the intestines by binding to bile acids. This phenomenon subsequently increases bile acid excretion and decreases cholesterol absorption from the intestines. These findings align with Kim et al. (2010), who reported that hesperetin reduced the hepatic lipid profile in hypercholesterolemic hamsters, resulting in reduced blood lipid levels.

We assessed the microscopic histological observations of the endocrine pancreas to learn whether biochemical modifications led to structural changes. The histological

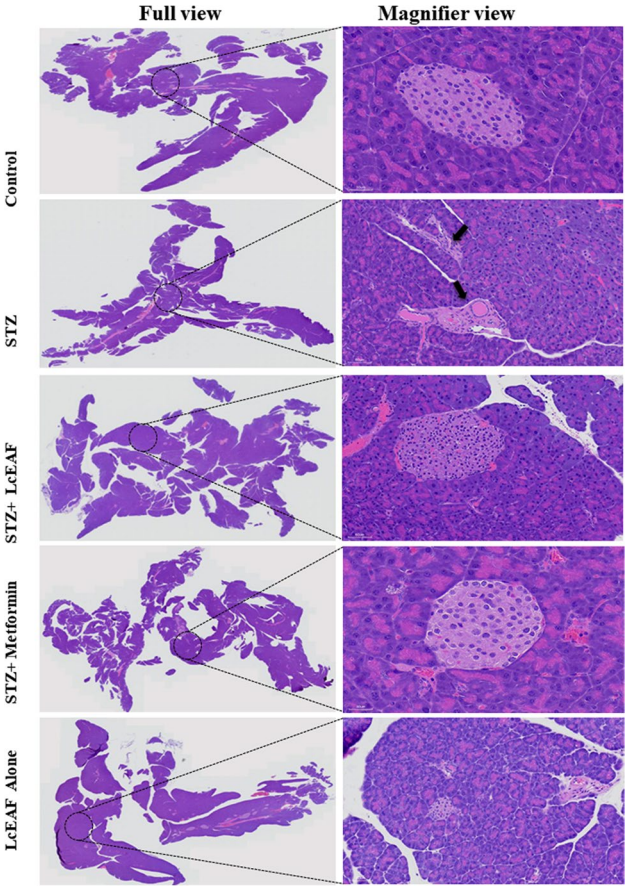

Fig. 5 Histopathological changes of the pancrease of STZ- and Lc-EAF-treated diabetic mice. Hematoxylin and eosin stain (H&E stain). Control and Lc-EAF alone-treated animal's pancreatic cells appeared as dense staining acini and a light-staining islet of Langerhans. STZ-treated animals show the infiltrated cells, which occur as the lymphocyte of immune system (dark blue dots) enters and destroys the beta cells (arrow). STZ with Lc-EAF showed a mild improvement in the pancreatic islet morphology. STZ + metformin-treated mice showed an improvement in the pancreatic islet morphology and improvement of the immune system

assessment of Lc-EAF-treated pancreatic tissue revealed significant improvement in both the changes in the islets and the numbers of pancreatic β-cells. The number of insulin-producing β-cells in STZ-injected ICR mice diminished, which lowered the amount of insulin in the blood. Interestingly, the application of Lc-EAF to STZ-induced ICR mice showed improvements in islet cell rejuvenation and increased insulin secretion, suggesting that Lc-EAF can defend and repair pancreatic β-cells from free radical exploitation (Fig. 5). Because of this, Lc-EAF could be of great help in helping to repair pancreatic β-cell damage and assist in the production of insulin. Increased glucose utilization in diabetic rats mediated by the promotion of β-cell regeneration and insulin secretion in the pancreas explains the antihyperglycemic effect of Lc-EAF.

Although the current experiment on diabetic rats has demonstrated hepatic damage as well, research also points to liver dysfunction and changes in circulating enzymes as additional contributors to hepatic injury. Decreased blood insulin, primarily due to leakage of these enzymes from the liver cytosol into the bloodstream, led to elevated ALT, AST, and ALP levels in the serum (Ollerton et al. 1999). Experimental ICR mice have significantly higher ALT, AST, and ALP levels than normal mice. Our results showed that administration of Lc-EAF prevented the rise in hepatic injury beyond normal levels, which may be due to the hepatoprotective effects of Lc-EAF (Table 7). Histological studies revealed that Lc-EAF improves cellular liver damage and successfully handles diabetic complications (Fig. 6).

Next, we found that blood urea nitrogen (BUN) and creatinine are excreted along with urea nitrogen in the urine. The presence of this waste product may indicate enhanced protein breakdown in both the liver and plasma in experimental diabetes (Ozcan et al. 2012). The current study discovered that elevated BUN levels are indicators of renal dysfunction in hyperglycemic mice. In diabetes, increased serum creatinine levels indicate a decreased GFR (Table 7). The findings of the present study suggest that Lc-EAF possesses the potential to attenuate renal injury caused by a hyperglycemic state, which is linked directly to the antioxidant capacity of the extract. Cutting-edge research on this particular extract and the present investigation highlights that it may be useful in treating diabetic nephropathy. The administration of Lc-EAF showed significantly improved STZ-induced histopathological changes in the kidneys of the ICR mice and minimal tubular damage and less necrotic damage (Fig. 7). The biochemical findings

Table 7 Influence of Lc-EAF in plasma ALT, AST, ALP, BUN, and creatinine level in control and experimental mice. The different superscript letters in the same column of the different group show the significant difference by Duncan's multiple range test ($p < 0.05$)

Group	ALT (U/L)	AST (U/L)	ALP (U/L)	BUN (mg/dL)	Creatinine (mg/dL)
Control	58.30 ± 4.98^{b}	42.06 ± 3.07^{a}	129.00 ± 10.58^{b}	39.36 ± 2.52^{b}	0.58 ± 0.05^{a}
STZ	134.87 ± 10.84^{d}	121.73 ± 8.02^{d}	227.86 ± 15.69^{d}	110.21 ± 6.41^{e}	2.32 ± 0.32^{c}
STZ + Lc-EAF	82.53 ± 5.54^{c}	60.24 ± 4.45^{c}	152.76 ± 2.16^{c}	64.23 ± 3.04^{c}	1.13 ± 0.13^{b}
STZ + metformin	62.53 ± 4.54^{b}	54.34 ± 3.65^{b}	124.65 ± 8.83^{b}	77.05 ± 4.76^{d}	1.25 ± 0.21^{b}
Lc-EAF alone	51.42 ± 3.30^{a}	43.08 ± 2.09^{a}	119.24 ± 7.51^{a}	33.52 ± 2.81^{a}	0.50 ± 0.05^{a}

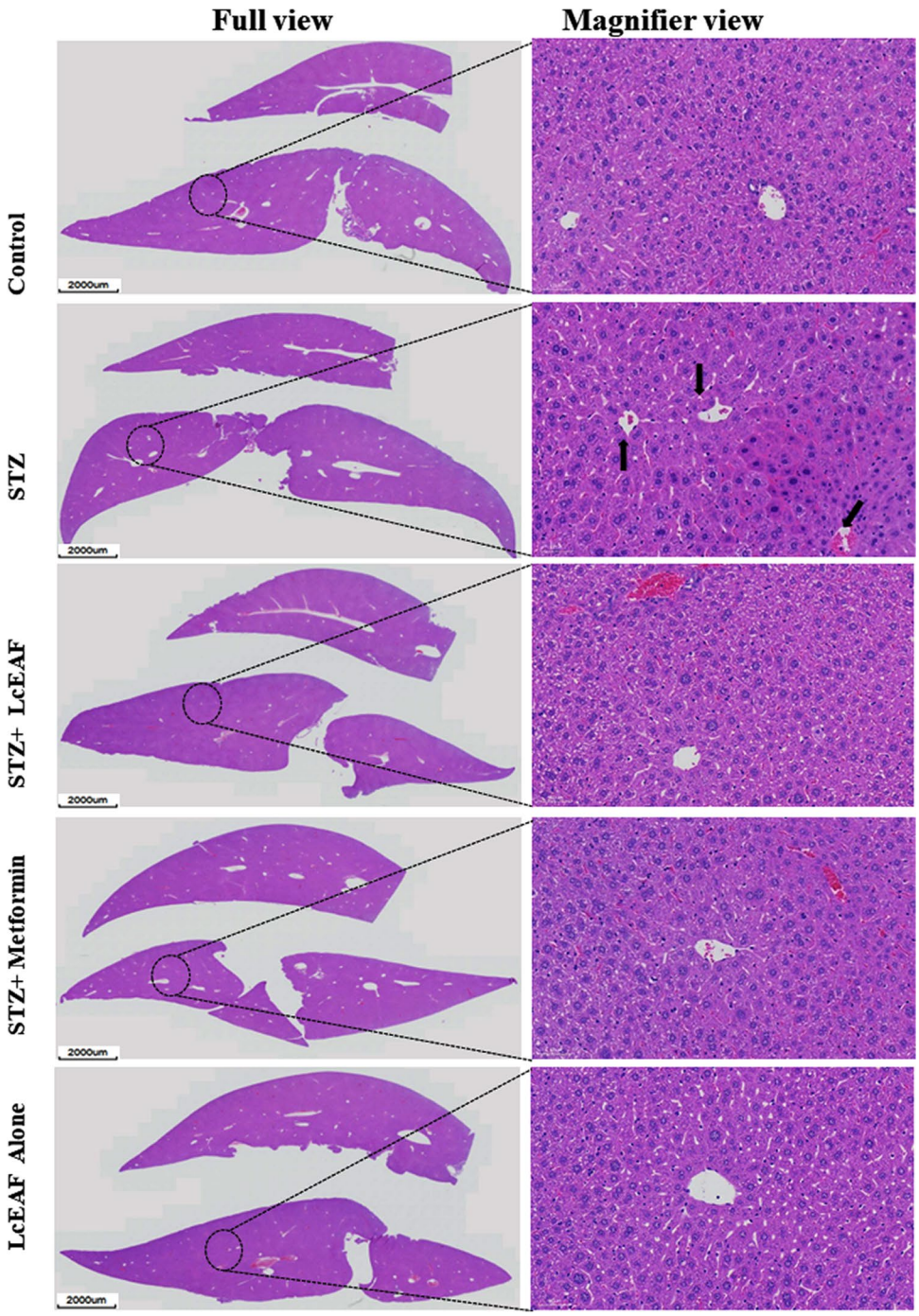

Fig. 6 Histopathological changes of the liver section of STZ- and Lc-EAF-treated diabetic mice (H&E stain). Control and Lc-EAF alone-treated animals showing a normal central vein and portal track appearance of liver cells. STZ-treated animals showed a fatty change, mild inflammatory infiltrate, and Mallory bodies due to degeneration of hepatocytes in diabetic rats (marked in arrow). Dilation and congestion of the central veins also appeared. STZ + metformin-treated animals showed a normal central vein and hepatocyte arrangement. STZ + Lc-EAF-treated animals showing a mild mononuclear inflammatory

corroborate histopathological findings and indicate the potential nephroprotective properties of Lc-EAF.

Conclusion

The ethyl acetate fraction of *Lespedeza cuneata* has a higher amount of polyphenols and flavonoids, favoring potent antioxidant and antidiabetic activities. From the Lc-EAF, 28 compounds were identified by UPLC-QTOF-MS/MS, including phenolics, flavonoids, lignans and triterpenoids. Among the identified phytochemical *trans-O*-coumaric acid 2-glucoside and glucosyringic acid has significant antidiabetic activity, it was revealed by molecular docking analysis. The mechanism of action of the Lc-EAF might be increasing insulin secretion and sensitivity in extract-treated diabetic mice. The findings will hopefully provide new insights into developing plant-derived antidiabetic drugs. It might pave the way for next-generation treatment for diabetes which might be less expensive and with minimum side effects. However, further research is

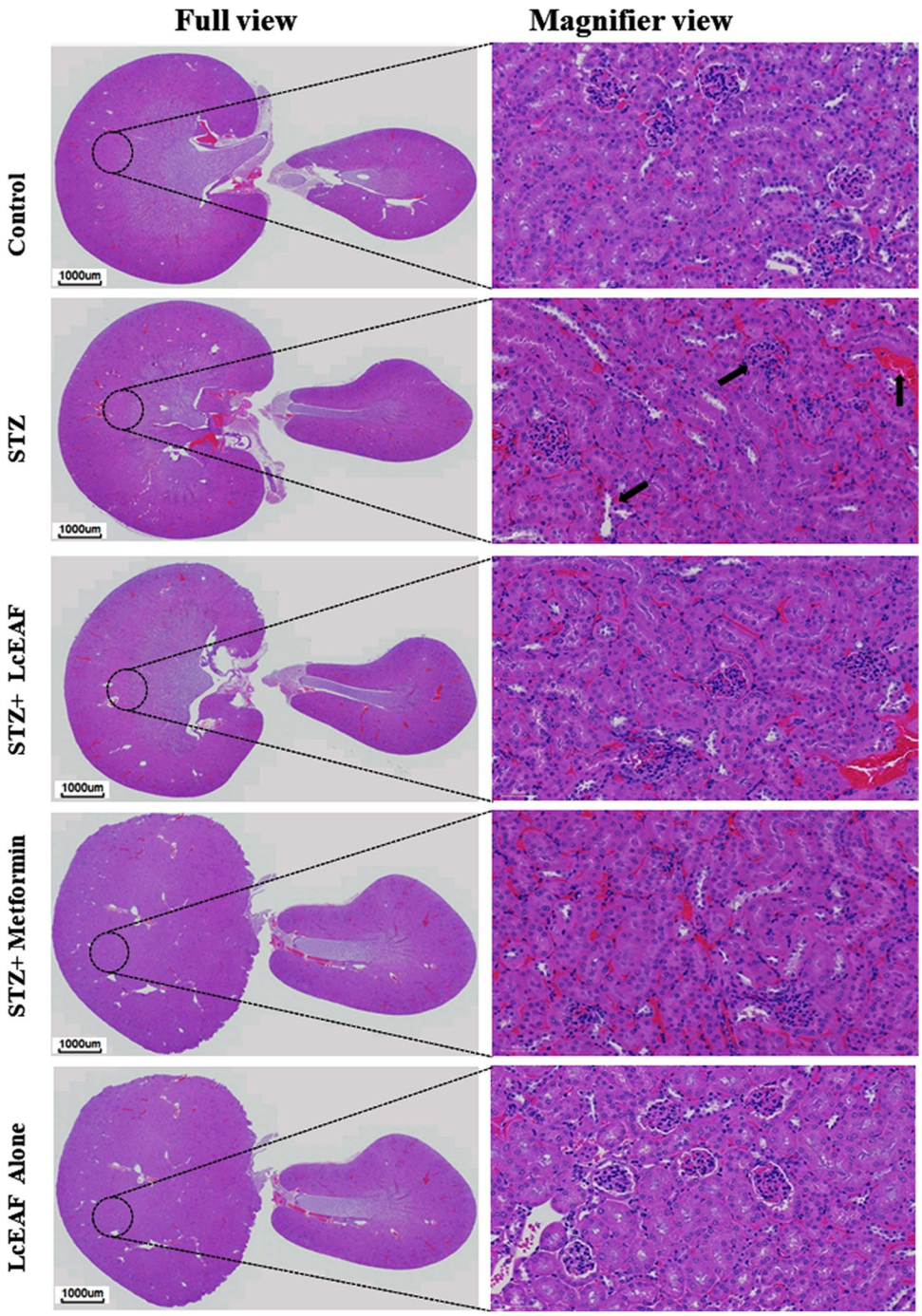

Fig. 7 Histopathological changes of the kidney of STZ- and Lc-EAF-treated diabetic mice (H&E stain). Control and Lc-EAF alone-treated animals showing a normal structure of glomeruli and tubules. STZ-treated animals showed lymphocyte infiltration in tubules and fatty infiltration (marked in arrow). STZ + metformin-treated animals showed glomeruli and renal tubule appear to be restored. STZ + Lc-EAF-treated animals showed a mild fatty infiltration with mild damage in renal tubules

essential to ascertain the active hypoglycemic components in *L. cuneate*, exclusively *trans*--coumaric acid 2-glucoside and glucosyringic acid.

Supplementary Information The online version contains supplementary material available at https://doi.org/10.1007/s11356-023-26412-8.

Author contribution Arokia Vijaya Anand Mariadoss: conceptualization, data curation, formal analysis, investigation, methodology, visualization, roles/writing-original draft, writing-review and editing. SeonJu Park: formal analysis, investigation. Kandasamy Saravanakumar: data curation, formal analysis, validation, review and editing. Anbazhagan Sathiyaseelan: software, formal analysis, data curation, validation. Myeong-Hyeon Wang: funding acquisition, project administration, resources, software, supervision, validation.

Funding This study was supported by the National Research Foundation of Korea (NRF) (2019R1A1055452; 2021R1I1A1A01057742; 2022R1A2C2091029; 2022R1F1A1063364).

Data availability The data are available from the corresponding author upon reasonable request and with permission of the study sponsor.

Declarations

Ethics approval All authors hereby declare that "Principles of Laboratory Animal Care" (NIH publication No. 85–23, revised 1985) were followed, as well as specific national laws where applicable. All animal experiments were performed under a protocol approved by the Local Institutional Animal Ethics Committee of Kangwon National University, Republic of Korea.

Consent to participate The authors agreed to participate in this work.

Consent for publication The work in this manuscript has not been previously published and is not under consideration of other journals.

Conflict of interest The authors declare no competing interests.

References

Ali MK, Seiglie JA, Narayan KMV (2021) Progress in diabetes prevention or epidemiology—or both, or neither? Lancet Diabetes Endocrinol 9:190

Anand Mariadoss AV, Krishnan Dhanabalan A, Munusamy H, Gunasekaran K, David E (2018) In silico studies towards enhancing the anticancer activity of phytochemical phloretin against cancer drug targets. Current Drug Therapy 13:174–188

Bender O, Llorent-Martínez EJ, Zengin G, Mollica A, Ceylan R, Molina-García L, Fernández-de Córdova ML, Atalay A (2018) Integration of in vitro and in silico perspectives to explain chemical characterization, biological potential and anticancer effects of Hypericum salsugineum: a pharmacologically active source for functional drug formulations. PLoS ONE 13:e0197815

Bianco A, Buiarelli F, Cartoni G, Coccioli F, Muzzalupo I, Polidori A, Uccella N (2001) Analysis by HPLC-MS/MS of biophenolic components in olives and oils. Anal Lett 34:1033–1051

Cantley J, Ashcroft FM (2015) Q&A: insulin secretion and type 2 diabetes: why do β-cells fail? BMC Biol 13:33–33

Cho EJ, Lee SG, Kim DO (2009) The effect of Lespedeza cuneata extract for antioxidative and whitening effect. J Life Resour Sci Res 28:34–38

Dineshkumar B, Mitra A, Manjunatha M (2010) A comparative study of alpha amylase inhibitory activities of common anti-diabetic plants at Kharagpur 1 block. Int J Green Pharm 4:115–121

Fernandes de Oliveira AM, Sousa Pinheiro L, Souto Pereira CK, Neves Matias W, Albuquerque Gomes R, Souza Chaves O, de Souza V, MdF N, de Almeida R, Simões de Assis T (2012) Total phenolic content and antioxidant activity of some Malvaceae family species. Antioxidants (basel, Switzerland) 1:33–43

Geng P, Sun J, Zhang M, Li X, Harnly JM, Chen P (2016) Comprehensive characterization of C-glycosyl flavones in wheat (Triticum aestivum L.) germ using UPLC-PDA-ESI/HRMS(n) and mass defect filtering. J Mass Spectrom: JMS 51:914–930

Guan L, Yang H, Cai Y, Sun L, Di P, Li W, Liu G, Tang Y (2019) ADMET-score–a comprehensive scoring function for evaluation of chemical drug-likeness. MedChemComm 10:148–157

Halliwell B, Gutteridge JMC, Aruoma OI (1987) The deoxyribose method: a simple "test-tube" assay for determination of rate constants for reactions of hydroxyl radicals. Anal Biochem 165:215–219

Honda M, Hara Y (1993) Inhibition of rat small intestinal sucrase and. ALPHA.-glucosidase activities by tea polyphenols. Biosci Biotechnol Biochem 57:123–124

Huneif MA, Alqahtani SM, Abdulwahab A, Almedhesh SA, Mahnashi MH, Riaz M, Ur-Rahman N, Jan MS, Ullah F, Aasim M, Sadiq A (2022) α-glucosidase, α-amylase andantioxidant evaluations of isolated bioactives from wild strawberry. Molecules 27:3444

Jeong MS, Park S, Han EJ, Park SY, Kim MJ, Jung K, Cho S-H, Kim S-Y, Yoon W-J, Ahn G, Kim K-N (2020) Pinus thunbergii PARL leaf protects against alcohol-induced liver disease by enhancing antioxidant defense mechanism in BALB/c mice. J Funct Foods 73:104116

Karar M, Kuhnert N (2015) UPLC-ESI-Q-TOF-MS/MS Characterization of phenolics from Crataegus monogyna and Crataegus laevigata (Hawthorn) leaves, fruits and their herbal derived drops (Crataegutt Tropfen). J Chem Biol Ther 1:102

Kaszás L, Alshaal T, El-Ramady H, Kovács Z, Koroknai J, Elhawat N, Nagy É, Cziáky Z, Fári M, Domokos-Szabolcsy É (2020) Identification of bioactive phytochemicals in leaf protein concentrate of Jerusalem artichoke (Helianthus tuberosus L). Plants 9:889

Khan MAB, Hashim MJ, King JK, Govender RD, Mustafa H, Al Kaabi J (2020) Epidemiology of type 2 diabetes - global burden of disease and forecasted trends. J Epidemiol Global Health 10:107–111

Khurana N, Ishar MPS, Gajbhiye A, Goel RK (2011) PASS assisted prediction and pharmacological evaluation of novel nicotinic analogs for nootropic activity in mice. Eur J Pharmacol 662:22–30

Kifayatullah M, Mustafa MS, Sengupta P, Sarker MMR, Das A, Das SK (2015) Evaluation of the acute and sub-acute toxicity of the ethanolic extract of Pericampylus glaucus (Lam.) Merr. in BALB/c mice. J Acute Dis 4:309–315

Kim S-J, Kim D-W (2007) Antioxidative activity of hot water and ethanol extracts of Lespedeza cuneata seeds. Korean J Food Preservation 14:332–335

Kim J-S, Kim M-J (2010) In vitro antioxidant activity of Lespedeza cuneata methanolic extracts. J Med Plants Res 4:674–679

Kim H-J, Jeon S-M, Lee M-K, Cho Y-Y, Kwon E-Y, Lee JH, Choi M-S (2010) Comparison of hesperetin and its metabolites for cholesterol-lowering and antioxidative efficacy in hypercholesterolemic hamsters. J Med Food 13:808–814

Kim SM, Kang K, Jho EH, Jung YJ, Nho CW, Um BH, Pan CH (2011) Hepatoprotective effect of flavonoid glycosides from Lespedeza cuneata against oxidative stress induced by tert-butyl hyperoxide. Phytother Res 25:1011–1017

Kumar S, Pandey AK (2013) Chemistry and biological activities of flavonoids: an overview. Sci World J 2013:162750

Lee H-J, Lim G-N, Park M-A, Park S-N (2011) Antibacterial and antioxidative activity of Lespedeza cuneata G. Don Extracts Microbiol Biotechnol Lett 39:63–69

Lee H, Jung JY, Hwangbo M, Ku SK, Kim YW, Jee SY (2013) Anti-inflammatory effects of Lespedeza cuneata *in vivo* and *in vitro*. Korea J Herbol 28:83–92

Lee JS, Lee AY, Quilantang NG, Geraldino PJL, Cho EJ, Lee S (2019) Antioxidant activity of avicularin and isovitexin from Lespedeza cuneata. J Appl Biol Chem 62:143–147

Li R, Liu S-k, Song W, Wang Y, Li Y-j, Qiao X, Liang H, Ye M (2014) Chemical analysis of the Tibetan herbal medicine Carduus acanthoides by UPLC/DAD/qTOF-MS and simultaneous determination of nine major compounds. Anal Methods 6:7181–7189

Lipinski CA (2004) Lead-and drug-like compounds: the rule-of-five revolution. Drug Discov Today Technol 1:337–341

Lipinski CA, Lombardo F, Dominy BW, Feeney PJ (1997) Experimental and computational approaches to estimate solubility and permeability in drug discovery and development settings. Adv Drug Deliv Rev 23:3–25

Liu S, Yu Z, Zhu H, Zhang W, Chen Y (2016) In vitro α-glucosidase inhibitory activity of isolated fractions from water extract of Qingzhuan dark tea. BMC Complement Altern Med 16:378–378

Magliano DJ, Chen L, Islam RM, Carstensen B, Gregg EW, Pavkov ME, Andes LJ, Balicer R, Baviera M, Boersma-van Dam E (2021) Trends in the incidence of diagnosed diabetes: a multicountry analysis of aggregate data from 22 million diagnoses in high-income and middle-income settings. Lancet Diabetes Endocrinol 9:203–211

Malik NH, Zin ZM, Razak SBA, Ibrahim K, Zainol MK (2017) Antioxidative activities and flavonoids contents in leaves of selected mangrove species in Setiu wetlands extracted using different solvents. J Sustain Sci Manag 3:14–22

Mariadoss AVA, Saravanakumar K, Sathiyaseelan A, Wang M-H (2020) Preparation, characterization and anti-cancer activity of graphene oxide–silver nanocomposite. J Photochem Photobiol B 210:111984

Mariadoss AVA, Park S, Saravanakumar K, Sathiyaseelan A, Wang M-H (2021) Ethyl acetate fraction of Helianthus tuberosus L. induces anti-diabetic, and wound-healing activities in insulin-resistant human liver cancer and mouse fibroblast cells. Antioxidants 10:99

Martín-Timón I, Sevillano-Collantes C, Segura-Galindo A, Del Cañizo-Gómez FJ (2014) Type 2 diabetes and cardiovascular disease: have all risk factors the same strength? World J Diabetes 5:444–470

Middleton E, Kandaswami C, Theoharides TC (2000) The effects of plant flavonoids on mammalian cells: implications for inflammation, heart disease, and cancer. Pharmacol Rev 52:673–751

Mirzaei M, Rahmaninan M, Mirzaei M, Nadjarzadeh A (2020) Epidemiology of diabetes mellitus, pre-diabetes, undiagnosed and uncontrolled diabetes in Central Iran: results from Yazd health study. BMC Public Health 20:166

Mohan V, Khunti K, Chan SP, Fadlo Filho F, Tran NQ, Ramaiya K, Joshi S, Mithal A, Mbaye MN, Nicodemus NA (2020) Management of type 2 diabetes in developing countries: balancing optimal glycaemic control and outcomes with affordability and accessibility to treatment. Diabetes Therapy 11:15–35

Nomura M, Takahashi T, Nagata N, Tsutsumi K, Kobayashi S, Akiba T, Yokogawa K, Moritani S, Miyamoto K-i (2008) Inhibitory mechanisms of flavonoids on insulin-stimulated glucose uptake in MC3T3-G2/PA6 adipose cells. Biol Pharm Bull 31:1403–1409

Oh S-H, Ku H, Park KS (2021) Prevalence and socioeconomic burden of diabetes mellitus in South Korean adults: a population-based study using administrative data. BMC Public Health 21:1–13

Ollerton RL, Playle R, Ahmed K, Dunstan FD, Luzio SD, Owens DR (1999) Day-to-day variability of fasting plasma glucose in newly diagnosed type 2 diabetic subjects. Diabetes Care 22:394–398

Oyaizu M (1986) Studies on products of browning reaction:antioxidative activities of product of browning reaction prepared from glucosamine. Japan J Nutr 44:307–315

Oyewande AA, Iqbal B, Abdalla LF, Karim F, Khan S (2020) An overview of the pathophysiology of metabolic changes and their sequence of occurrence in obese diabetic females: a narrative review. Cureus 12:e10947

Ozcan F, Ozmen A, Akkaya B, Aliciguzel Y, Aslan M (2012) Beneficial effect of myricetin on renal functions in streptozotocin-induced diabetes. Clin Exp Med 12:265–272

Park Y-I, Cha YE, Jang M, Park R, Namkoong S, Kwak J, Jang I-S, Park J (2020) The flower extract of Abelmoschus manihot (Linn.) increases cyclin d1 expression and activates cell proliferation. J Microbiol Biotechnol 30:1044–1050

Piraud M, Vianey-Saban C, Petritis K, Elfakir C, Steghens J-P, Morla A, Bouchu D (2003) ESI-MS/MS analysis of underivatised amino acids: a new tool for the diagnosis of inherited disorders of amino acid metabolism. Fragmentation study of 79 molecules of biological interest in positive and negative ionisation mode. Rapid Commun Mass Spectrom 17:1297–1311

Poovitha S, Parani M (2016) In vitro and *in vivo* α-amylase and α-glucosidase inhibiting activities of the protein extracts from two varieties of bitter gourd (Momordica charantia L). BMC Complement Altern Med 16:185

Qin N, Chen Y, Jin M-N, Zhang C, Qiao W, Yue X-L, Duan H-Q, Niu W-Y (2016) Anti-obesity and antidiabetic effects of flavonoid derivative (Fla-CN) via microRNA in high fat diet induced obesity mice. Eur J Pharm Sci 82:52–63

Rahmati M, Gharakhanlou R, Movahedin M, Mowla SJ, Khazani A, Fouladvand M, Golbar SJ (2015) Treadmill training modifies KIF5B motor protein in the STZ-induced diabetic rat spinal cord and sciatic nerve. Arch Iran Med 18:94–101

Röder PV, Wu B, Liu Y, Han W (2016) Pancreatic regulation of glucose homeostasis. Exp Mol Med 48:e219–e219

Rohn S, Rawel HM, Kroll J (2002) Inhibitory effects of plant phenols on the activity of selected enzymes. J Agric Food Chem 50:3566–3571

Ruan J, Yan J, Zheng D, Sun F, Wang J, Han L, Zhang Y, Wang T (2019) Comprehensive chemical profiling in the ethanol extract of Pluchea indica aerial parts by liquid chromatography/mass spectrometry analysis of its silica gel column chromatography fractions. Molecules (basel, Switzerland) 24:2784

Saadane A, Lessieur EM, Du Y, Liu H, Kern TS (2020) Successful induction of diabetes in mice demonstrates no gender difference in development of early diabetic retinopathy. PLoS ONE 15:e0238727–e0238727

Saravanakumar K, Sathiyaseelan A, Mariadoss AVA, Wang M-H (2021) Antioxidant and antidiabetic properties of biocompatible ceria oxide (CeO2) nanoparticles in mouse fibroblast NIH3T3 and insulin resistant HepG2 cells. Ceram Int 47:8618–8626

Sharma BR, Kim MS, Yokozawa T, Rhyu DY (2014) Antioxidant and antidiabetic activities of Lespedeza cuneata water extract. J Med Plants Res 8:935–941

Singleton VL, Orthofer R, Lamuela-Raventós RM (1999) Analysis of total phenols and other oxidation substrates and antioxidants by means of Folin-Ciocalteu reagent. Methods Enzymol 299:152–178

Srinivasan S, Pari L (2013) Antihyperlipidemic effect of diosmin: a citrus flavonoid on lipid metabolism in experimental diabetic rats. J Funct Foods 5:484–492

Sudha P, Zinjarde SS, Bhargava SY, Kumar AR (2011) Potent α-amylase inhibitory activity of Indian Ayurvedic medicinal plants. BMC Complement Altern Med 11:1–10

Sun C et al (2020) Dietary polyphenols as antidiabetic agents: advances and opportunities. Food Frontiers 1:18–44

Sun H, Saeedi P, Karuranga S, Pinkepank M, Ogurtsova K, Duncan BB, Stein C, Basit A, Chan JC, Mbanya JCJDR (2022) IDF Diabetes Atlas: global, regional and country-level diabetes prevalence estimates for 2021 and projections for 2045. Diabetes Res Clin Pract 183:109119

Tshiyoyo KS, Bester MJ, Serem JC, Apostolides Z (2022) In-silico reverse docking and in-vitro studies identified curcumin, 18α-glycyrrhetinic acid, rosmarinic acid, and quercetin as inhibitors of α-glucosidase and pancreatic α-amylase and lipid accumulation in HepG2 cells, important type 2 diabetes targets. J Mol Str 1266:133492

Unuofin JO, Otunola GA, Afolayan AJ (2017) Phytochemical screening and in vitro evaluation of antioxidant and antimicrobial activities of Kedrostis africana (L.) Cogn. Asian Pac J Trop Biomed 7:901–908

Vinayagam R, Jayachandran M, Xu B (2016) Antidiabetic effects of simple phenolic acids: a comprehensive review. Phytother Res 30:184–199

Vinayagam R, Xiao J, Xu B (2017) An insight into antidiabetic properties of dietary phytochemicals. Phytochem Rev 16:535–553

Virgen-Ortíz JJ, Ibarra-Junquera V, Escalante-Minakata P, Centeno-Leija S, Serrano-Posada H, de Jesús O-P, Pérez-Martínez JD, Osuna-Castro JA (2016) Identification and functional

characterization of a fructooligosaccharides-forming enzyme from Aspergillus aculeatus. Appl Biochem Biotechnol 179:497–513
Wang Y, Xiang L, Wang C, Tang C, He X (2013) Antidiabetic and antioxidant effects and phytochemicals of mulberry fruit (Morus alba L.) polyphenol enhanced extract. PLoS ONE 8:e71144–e71144
Wang Y, Wu S, Wen F, Cao Q (2020) Diabetes mellitus as a risk factor for retinal vein occlusion: a meta-analysis. Medicine 99:e19319
Yoo G, Park SJ, Lee TH, Yang H, Baek Y-s, Kim N, Kim YJ, Kim SH (2015) Flavonoids isolated from Lespedeza cuneata G. Don and their inhibitory effects on nitric oxide production in lipopolysaccharide-stimulated BV-2 microglia cells. Pharmacogn Mag 11:651
Zakaria Z, Aziz R, Lachimanan YL, Sreenivasan S, Rathinam X (2008) Antioxidant activity of Coleus blumei, Orthosiphon stamineus, Ocimum basilicum and Mentha arvensis from Lamiaceae family. Int J Nat Eng Sci 2:93–95
Zhang C, Zhou J, Yang J, Li C, Ma J, Zhang D, Zhang D (2016) Two new phenylpropanoid glycosides from the aerial parts of Lespedeza cuneata. Acta Pharmaceutica Sinica B 6:564–567
Zhang L, Tu Z-c, Xie X, Wang H, Wang H, Wang Z-x, Sha X-m, Lu Y (2017) Jackfruit (Artocarpus heterophyllus Lam.) peel: a better source of antioxidants and a-glucosidase inhibitors than pulp, flake and seed, and phytochemical profile by HPLC-QTOF-MS/MS. Food Chem 234:303–313
Zhishen J, Mengcheng T, Jianming W (1999) The determination of flavonoid contents in mulberry and their scavenging effects on superoxide radicals. Food Chem 64:555–559
Zhou J, Zheng X, Yang Q, Liang Z, Li D, Yang X, Xu J (2013) Optimization of ultrasonic-assisted extraction and radical-scavenging capacity of phenols and flavonoids from Clerodendrum cyrtophyllum Turcz leaves. PLoS ONE 8:e68392
Zhou J, Li C-J, Yang J-Z, Ma J, Wu L-Q, Wang W-J, Zhang D-M (2016) Phenylpropanoid and lignan glycosides from the aerial parts of Lespedeza cuneata. Phytochemistry 121:58–64
Donato MT, Tolosa L, Gómez-Lechón MJ (2015) Culture and functional characterization of human hepatoma HepG2 cells, Protocols in In Vitro Hepatocyte Research. Springer, pp. 77–93